


# Basic Principles of Homing Guidance

Neil F. Palumbo, Ross A. Blauwkamp,  
and Justin M. Lloyd



This article provides a conceptual foundation with respect to homing guidance upon which the next several articles are anchored. To this end, a basic geometric and notational framework is first established. Then, the well-known and often-used proportional navigation guidance concept is developed. The mechanization of proportional navigation in guided missiles depends on several factors, including the types of inertial and target sensors available on board the missile. Within this context, the line-of-sight reconstruction process (the collection and orchestration of the inertial and target sensor measurements necessary to support homing guidance) is discussed. Also, guided missiles typically have no direct control over longitudinal acceleration, and they maneuver in the direction specified by the guidance law by producing acceleration normal to the missile body. Therefore, we discuss a guidance command preservation technique that addresses this lack of control. The key challenges associated with designing effective homing guidance systems are discussed, followed by a cursory discussion of midcourse guidance for completeness' sake.

## INTRODUCTION

The key objective of this article is to provide a broad conceptual foundation with respect to homing guidance but with sufficient depth to adequately support the articles that follow. During guidance analysis, it is typical to assume that the missile is on a near-collision course with the target. The implications of this and other assumptions are discussed in the first section, *Handover Analysis*.

The next section, *Engagement Kinematics*, establishes a geometric foundation for analysis that is used in the subsequent sections of this and the other guidance-related articles in this issue. In particular, a line-of-sight (LOS) coordinate frame is introduced upon which the kinematic equations of motion are developed; this coordinate frame supports the subsequent derivation of

proportional navigation (PN) guidance. Over the past 50 years, PN has proven both reliable and robust, thereby contributing to its continued use. The *Development of PN Guidance Law* section presents the derivation of and discusses this popular and much-used technique. The subsequent section, *Mechanization of PN*, discusses how PN may be implemented in a homing missile. Key drivers here are the type of sensor that is used to detect and track the target, how the sensor is mounted to the missile, and how the LOS (rate) measurement is developed. The next section, *Radome/Irdome Design Requirements*, briefly discusses the functional requirements imposed on modern missile radomes. This is followed by an expanded section on *Guidance System Design Challenges*. Here, the contributors to the degradation of guidance system performance (radome error and others) are discussed. Then, *Guidance Command Preservation* presents a technique for commanding acceleration commands perpendicular to the missile body that will effectively maneuver the missile in the desired guidance direction. Although this article is mainly concerned with terminal homing concepts, the *Midcourse Guidance* section briefly discusses issues and requirements associated with the midcourse phase of flight.

### Handover Analysis

When terminal guidance concepts are being developed or related systems analysis is being performed, it typically is assumed that the missile interceptor is on a collision course (or nearly so) with the target. In reality, this is not usually the case. For example, there can be significant uncertainty in target localization, particularly early in the engagement process, that precludes satisfaction of a collision course condition prior to terminal homing. Moreover, the unpredictable nature of future target maneuvers (e.g., target booster staging events, energy management steering, coning of a ballistic missile reentry vehicle, or the weaving or spiraling maneuvers of an anti-ship cruise missile) can complicate the development of targeting, launch, and/or (midcourse) guidance solutions that guarantee collision course conditions before initiation of terminal homing. In addition, cumulative errors are associated with missile navigation and the effects of unmodeled missile dynamics that all add together to complicate satisfaction of a collision course condition. For simplicity, all of these errors can be collectively regarded as uncertainties in the location of the target with respect to the missile interceptor. Thus, if the interceptor is launched (and subsequently guided during midcourse) on the basis of estimated (predicted) future target position, then, at the time of acquisition by the onboard seeker, the actual target position will be displaced from its predicted position. Figure 1 notionally illustrates this condition, where  $\bar{\mathbf{r}}$  is the LOS vector between the missile and the predicted target location;

$\bar{\mathbf{I}}_{r_{LOS}} = \bar{\mathbf{r}}/\|\bar{\mathbf{r}}\|$  is the unit vector along the LOS;  $\bar{\mathbf{v}}_T$  and  $\bar{\mathbf{v}}_M$  are the velocity vectors of the target and missile, respectively;  $\bar{\mathbf{v}}_R = \bar{\mathbf{v}}_T - \bar{\mathbf{v}}_M$  is the relative velocity vector; and  $\bar{\mathbf{e}}$  is the displacement error between predicted and true target position.

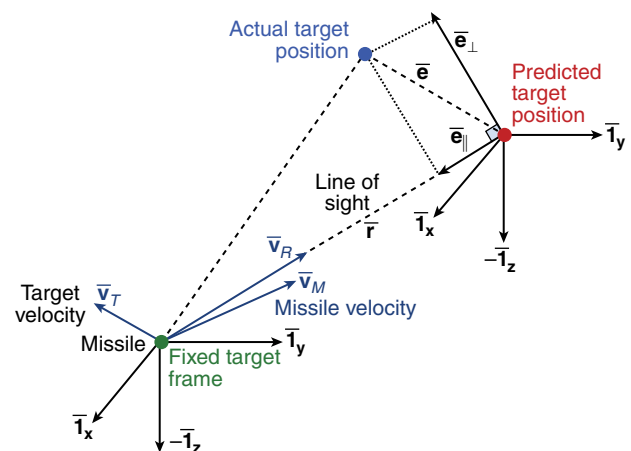
As discussed, ideally, the relative velocity vector is along the LOS to the true future target position (at the time of intercept). However, Fig. 1 depicts a more realistic condition where the relative velocity is along the LOS to the estimated future target position in space. For this case, the interceptor will miss the target unless it applies corrective maneuvers.

Figure 1 illustrates that the displacement error,  $\bar{\mathbf{e}}$ , can be decomposed into two components: one along ( $\bar{\mathbf{e}}_{\parallel}$ ) and one perpendicular ( $\bar{\mathbf{e}}_{\perp}$ ) to the predicted target LOS. This decomposition is expressed in Eq. 1:

$$\begin{aligned} \bar{\mathbf{e}}_{\parallel} &= (\bar{\mathbf{e}} \cdot \bar{\mathbf{I}}_{r_{LOS}}) \bar{\mathbf{I}}_{r_{LOS}} \\ \bar{\mathbf{e}}_{\perp} &= \bar{\mathbf{I}}_{r_{LOS}} \times (\bar{\mathbf{e}} \times \bar{\mathbf{I}}_{r_{LOS}}). \end{aligned} \tag{1}$$

In this equation,  $\bar{\mathbf{x}} \cdot \bar{\mathbf{y}}$  represents the dot (scalar) product between the two vectors  $\bar{\mathbf{x}}$  and  $\bar{\mathbf{y}}$ , and  $\bar{\mathbf{x}} \times \bar{\mathbf{y}}$  represents the cross (vector) product between the two vectors. Note that, because the relative velocity vector,  $\bar{\mathbf{v}}$ , is along the LOS to the predicted target location, the error  $\bar{\mathbf{e}}_{\parallel}$  will alter the time of intercept but does not contribute to the final miss distance. Consequently, the miss distance that must be removed by the interceptor after transition to terminal homing is contained in  $\bar{\mathbf{e}}_{\perp}$  (i.e., target uncertainty normal to the LOS).

Homing missile guidance strategies (guidance laws) dictate the manner in which the missile will guide to intercept, or rendezvous with, the target. The feedback nature of homing guidance allows the guided missile (or, more generally, “the pursuer”) to tolerate some



**Figure 1.** To assist in simplifying the analysis of handover to terminal homing, all of the contributing navigation and engagement modeling errors are collectively regarded as uncertainties to the location of the target with respect to the missile at handover.

level of (sensor) measurement uncertainties, errors in the assumptions used to model the engagement (e.g., unanticipated target maneuver), and errors in modeling missile capability (e.g., deviation of actual missile speed of response to guidance commands from the design assumptions). Nevertheless, the selection of a guidance strategy and its subsequent mechanization are crucial design factors that can have substantial impact on guided missile performance. Key drivers to guidance law design include the type of targeting sensor to be used (passive IR, active or semi-active RF, etc.), accuracy of the targeting and inertial measurement unit (IMU) sensors, missile maneuverability, and, finally yet important, the types of targets to be engaged and their associated maneuverability levels. We will begin by developing a basic model of the engagement kinematics. This will lay the foundation upon which PN, one of the oldest and most common homing missile guidance strategies, is introduced.

### Engagement Kinematics: The Line-of-Sight Coordinate System

The development presented here follows the one given in Ref. 1. In the sequel, the following notation is used:  $\mathbf{X} = n \times m$  (read  $n$ -by- $m$ ) matrix of scalar elements  $x_{i,j}$ ,  $i = 1 \dots n$ ,  $j = 1 \dots m$ ;  $\bar{\mathbf{x}} = n \times 1$  vector of scalar elements  $x_i$ ,  $i = 1 \dots n$ ;  $\|\bar{\mathbf{x}}\| = \sqrt{\sum_{i=1}^n x_i^2}$  = Euclidean vector norm of  $\bar{\mathbf{x}}$ ;  $\bar{\mathbf{1}}_x = \bar{\mathbf{x}}/\|\bar{\mathbf{x}}\| = n \times 1$  unit vector (e.g.,  $\|\bar{\mathbf{1}}_x\| = 1$ ) in the direction of  $\bar{\mathbf{x}}$ ;  $\delta/\delta t$  = time derivative with respect to a fixed (inertial) coordinate system; and  $d/dt$  = time derivative with respect to a rotating coordinate system.

Consider the engagement geometry shown in Fig. 2, where  $\bar{\mathbf{r}}_M$  and  $\bar{\mathbf{r}}_T$  are the position vectors of the missile interceptor and target with respect to a fixed coordinate frame of reference (represented by the triad  $\{\bar{\mathbf{1}}_x, \bar{\mathbf{1}}_y, \bar{\mathbf{1}}_z\}$ ). Consequently, we define the relative position vector of the target with respect to the missile as shown in Eq. 2:

$$\bar{\mathbf{r}} = \bar{\mathbf{r}}_T - \bar{\mathbf{r}}_M. \quad (2)$$

The relative position vector can be written as  $\bar{\mathbf{r}} = R\bar{\mathbf{1}}_r$ , where  $R = \|\bar{\mathbf{r}}\|$  is the target–missile range, and  $\bar{\mathbf{1}}_r$  is the unit vector directed along  $\bar{\mathbf{r}}$  (we refer to  $\bar{\mathbf{1}}_r$  as the LOS unit vector). Differentiating the relative position vector,  $\dot{\bar{\mathbf{r}}} = \dot{R}\bar{\mathbf{1}}_r + R\dot{\bar{\mathbf{1}}}_r$ , with respect to the fixed coordinate system, we obtain the following expression for relative velocity  $\bar{\mathbf{v}}$ :

$$\bar{\mathbf{v}} \equiv \frac{\delta}{\delta t} \bar{\mathbf{r}} = \dot{R}\bar{\mathbf{1}}_r + R \frac{\delta}{\delta t} \bar{\mathbf{1}}_r. \quad (3)$$

From Eq. 3, one can see that the rate of change of the relative position vector (i.e., relative velocity) comprises two components: (i) a change in  $\bar{\mathbf{r}}$  as a result of a change in length ( $\dot{R}$ ) and (ii) a change in direction (a rotation) as a result of the rate of change of the LOS unit vector.

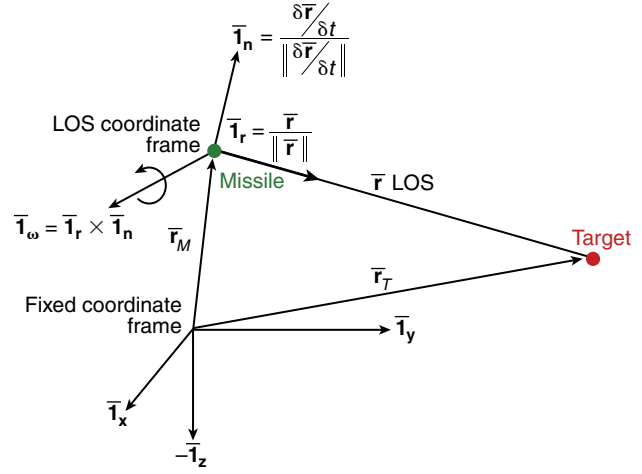


**Figure 2.** In the LOS coordinate frame, the LOS rate is perpendicular to the LOS direction and rotation of the LOS takes place about the  $\bar{\mathbf{1}}_\omega$ .

We define this change in direction by the vector  $\bar{\mathbf{n}}$  as given in Eq. 4:

$$\bar{\mathbf{n}} \equiv \frac{\delta}{\delta t} \bar{\mathbf{1}}_r. \quad (4)$$

Consequently, a second unit vector,  $\bar{\mathbf{1}}_n$ , is defined to be in the direction of  $\bar{\mathbf{n}}$  as shown:

$$\bar{\mathbf{1}}_n = \frac{\delta \bar{\mathbf{1}}_r / \delta t}{\|\delta \bar{\mathbf{1}}_r / \delta t\|} = \frac{\bar{\mathbf{n}}}{\|\bar{\mathbf{n}}\|}. \quad (5)$$

Finally, to complete the definition of the (right-handed) LOS coordinate system, a third unit vector,  $\bar{\mathbf{1}}_\omega$ , is defined as the cross product of the first two:

$$\bar{\mathbf{1}}_\omega = \bar{\mathbf{1}}_r \times \bar{\mathbf{1}}_n. \quad (6)$$

In general, the angular velocity of the LOS coordinate system with respect to an inertial reference frame is given by  $\dot{\bar{\varphi}} = \dot{\phi}_r \bar{\mathbf{1}}_r + \dot{\phi}_n \bar{\mathbf{1}}_n + \dot{\phi}_\omega \bar{\mathbf{1}}_\omega$ , where the components of the angular velocity are given in Eq. 7:

$$\begin{aligned} \dot{\phi}_r &= \dot{\bar{\varphi}} \cdot \bar{\mathbf{1}}_r \\ \dot{\phi}_n &= \dot{\bar{\varphi}} \cdot \bar{\mathbf{1}}_n \\ \dot{\phi}_\omega &= \dot{\bar{\varphi}} \cdot \bar{\mathbf{1}}_\omega. \end{aligned} \quad (7)$$

Thus, upon reexamination of Eq. 4, we note that the LOS rate,  $\bar{\mathbf{n}}$ , can be expressed as shown in Eq. 8:

$$\bar{\mathbf{n}} = \frac{d}{dt} \bar{\mathbf{1}}_r + \dot{\bar{\varphi}} \times \bar{\mathbf{1}}_r. \quad (8)$$

On the right-hand side of Eq. 8, the expression  $d\bar{\mathbf{1}}_r/dt$  represents the time derivative of the LOS unit vector with respect to a rotating coordinate frame, and  $\dot{\bar{\varphi}}$  is

the angular velocity of the rotating frame with respect to the inertial frame. The former component is equal to zero (i.e., the LOS unit vector is a constant). Therefore, the LOS rate and corresponding unit vectors simplify to the following expressions:

$$\begin{aligned}\bar{\mathbf{n}} &= \dot{\bar{\varphi}} \times \bar{\mathbf{I}}_r \\ \bar{\mathbf{I}}_n &= \frac{\dot{\bar{\varphi}} \times \bar{\mathbf{I}}_r}{\|\dot{\bar{\varphi}} \times \bar{\mathbf{I}}_r\|}.\end{aligned}\quad (9)$$

Thus, from Eq. 3, the relative velocity expression is given as

$$\bar{\mathbf{v}} = \dot{R}\bar{\mathbf{I}}_r + R(\dot{\bar{\varphi}} \times \bar{\mathbf{I}}_r). \quad (10)$$

The typical guided missile control variable is interceptor acceleration. Thus, taking the derivative of Eq. 10, and using Eq. 9, we obtain an expression for the relative acceleration:

$$\begin{aligned}\frac{\delta}{\delta t}\bar{\mathbf{v}} &= \ddot{R}\bar{\mathbf{I}}_r + \dot{R}\frac{\delta}{\delta t}\bar{\mathbf{I}}_r + \dot{R}(\dot{\bar{\varphi}} \times \bar{\mathbf{I}}_r) + R(\ddot{\bar{\varphi}} \times \bar{\mathbf{I}}_r) + R(\dot{\bar{\varphi}} \times \frac{\delta}{\delta t}\bar{\mathbf{I}}_r) \\ &= \ddot{R}\bar{\mathbf{I}}_r + 2\dot{R}(\dot{\bar{\varphi}} \times \bar{\mathbf{I}}_r) + R(\ddot{\bar{\varphi}} \times \bar{\mathbf{I}}_r) + R[\dot{\bar{\varphi}} \times (\dot{\bar{\varphi}} \times \bar{\mathbf{I}}_r)].\end{aligned}\quad (11)$$

Next, using the definition of  $\dot{\bar{\varphi}}$  in Eq. 7 and the fact that  $\bar{\mathbf{I}}_r = [1 \ 0 \ 0]^T$ , we expand the term  $\dot{\bar{\varphi}} \times \bar{\mathbf{I}}_r \equiv \bar{\mathbf{n}}$  in Eq. 11, which results in the following relation:

$$\dot{\bar{\varphi}} \times \bar{\mathbf{I}}_r = \det \begin{vmatrix} \bar{\mathbf{I}}_r & \bar{\mathbf{I}}_n & \bar{\mathbf{I}}_\omega \\ \dot{\bar{\varphi}}_r & \dot{\bar{\varphi}}_n & \dot{\bar{\varphi}}_\omega \\ 1 & 0 & 0 \end{vmatrix} = \dot{\bar{\varphi}}_\omega \bar{\mathbf{I}}_n - \dot{\bar{\varphi}}_n \bar{\mathbf{I}}_\omega. \quad (12)$$

Here,  $\det|\cdot|$  represents taking the determinant of a matrix. From Eq. 4, the direction of  $\bar{\mathbf{n}}$  can have no component along  $\bar{\mathbf{I}}_\omega$ . Thus, we conclude  $\dot{\bar{\varphi}}_n = 0$  and obtain the result in Eq. 13:

$$\dot{\bar{\varphi}} \times \bar{\mathbf{I}}_r = \dot{\bar{\varphi}}_\omega \bar{\mathbf{I}}_n. \quad (13)$$

In Eq. 13,  $\dot{\bar{\varphi}}_\omega \equiv \|\bar{\mathbf{n}}\|$ . Using Eq. 13, the other cross-product terms in Eq. 11 yield the following results:

$$\begin{aligned}\dot{\bar{\varphi}} \times (\dot{\bar{\varphi}} \times \bar{\mathbf{I}}_r) &= -\dot{\bar{\varphi}}_\omega^2 \bar{\mathbf{I}}_r + \dot{\bar{\varphi}}_r \dot{\bar{\varphi}}_\omega \bar{\mathbf{I}}_\omega \\ \ddot{\bar{\varphi}} \times \bar{\mathbf{I}}_r &= \ddot{\bar{\varphi}}_\omega \bar{\mathbf{I}}_n.\end{aligned}\quad (14)$$

Using Eqs. 13 and 14 in Eq. 11, we obtain the desired expression for relative acceleration:

$$\begin{aligned}\frac{\delta^2}{\delta t^2}\bar{\mathbf{r}} &= \bar{\mathbf{a}}_T - \bar{\mathbf{a}}_M \\ &= (\ddot{R} - R\dot{\bar{\varphi}}_\omega^2)\bar{\mathbf{I}}_r + (2\dot{R}\dot{\bar{\varphi}}_\omega + R\ddot{\bar{\varphi}}_\omega)\bar{\mathbf{I}}_n + (R\dot{\bar{\varphi}}_\omega\dot{\bar{\varphi}}_r)\bar{\mathbf{I}}_\omega.\end{aligned}\quad (15)$$

From Eq. 15, the components of relative acceleration in the LOS coordinate frame can be written as shown in Eq. 16:

$$\begin{aligned}(\bar{\mathbf{a}}_T - \bar{\mathbf{a}}_M) \cdot \bar{\mathbf{I}}_r &= \ddot{R} - R\dot{\bar{\varphi}}_\omega^2 \\ (\bar{\mathbf{a}}_T - \bar{\mathbf{a}}_M) \cdot \bar{\mathbf{I}}_n &= 2\dot{R}\dot{\bar{\varphi}}_\omega + R\ddot{\bar{\varphi}}_\omega \\ (\bar{\mathbf{a}}_T - \bar{\mathbf{a}}_M) \cdot \bar{\mathbf{I}}_\omega &= R\dot{\bar{\varphi}}_\omega\dot{\bar{\varphi}}_r.\end{aligned}\quad (16)$$

### Development of PN Guidance Law

Many guided missiles employ some version of PN as the guidance law during the terminal homing phase. Surface-to-air, air-to-air, and air-to-surface missile engagements, as well as space applications (including rendezvous), use PN in one form or another as a guidance law.<sup>1-7</sup> A major advantage of PN, contributing to its longevity as a favored guidance scheme over the last five decades, is its relative simplicity of implementation. The most basic PN implementations require low levels of information regarding target motion as compared with other more elaborate schemes (some are discussed in the next article in this issue, “Modern Homing Missile Guidance Theory and Techniques”), thus simplifying onboard sensor requirements. Moreover, it has proven to be relatively reliable and robust. As also will be seen in the next article in this issue, under certain conditions and (simplifying) assumptions about target and missile characteristics, the PN law is an optimal guidance strategy in the sense of minimizing the terminal miss distance.

In order to develop the PN guidance strategy, we first look to the components of Eq. 16 for sufficient conditions to achieve an intercept. Looking at the first component, sufficient conditions for an intercept are (i) the LOS rate is zero ( $\dot{\bar{\varphi}}_\omega = 0$ ), (ii) interceptor capability to accelerate along the LOS is greater than or equal to target acceleration along the LOS ( $\bar{\mathbf{a}}_M \cdot \bar{\mathbf{I}}_r \geq \bar{\mathbf{a}}_T \cdot \bar{\mathbf{I}}_r$ ), and (iii) the initial range rate along the LOS is negative ( $\dot{R}(0) < 0$ ). In this case, missile-to-target range ( $R$ ) will decrease linearly ( $(\bar{\mathbf{a}}_T - \bar{\mathbf{a}}_M) \cdot \bar{\mathbf{I}}_r = 0$ ) or quadratically ( $(\bar{\mathbf{a}}_T - \bar{\mathbf{a}}_M) \cdot \bar{\mathbf{I}}_r < 0$ ) with respect to time and, eventually, pass through zero.

From the discussion above, the interceptor must accelerate such as to null the LOS rate ( $\dot{\bar{\varphi}}_\omega$ ). We look to the second component of Eq. 16 to determine how this can be done. We first define closing velocity as  $V_c \equiv -\dot{R}$ . Note that for an approaching trajectory  $\dot{R} < 0$ ; thus  $V_c > 0$ . If, for the moment, we treat closing velocity and range as constant, then taking the Laplace transform of the second component of Eq. 16 yields the following polynomial in  $s$ :

$$(\bar{\mathbf{a}}_T(s) - \bar{\mathbf{a}}_M(s)) \cdot \bar{\mathbf{I}}_n = (sR - 2V_c)\dot{\bar{\varphi}}_\omega(s). \quad (17)$$

In Eq. 17,  $s$  represents the Laplace transform variable. Thus, if we define interceptor acceleration perpendicular to the LOS to be  $\bar{\mathbf{a}}_M(s) \cdot \bar{\mathbf{I}}_n = \Lambda\dot{\bar{\varphi}}_\omega(s)$ , then, from Eq. 17, we can write the transfer function from target accelera-



tion (perpendicular to the LOS) to the corresponding LOS rate:

$$\frac{\dot{\phi}_{\omega}(s)}{(\bar{\mathbf{a}}_T(s) \cdot \bar{\mathbf{I}}_n)} = \frac{1}{(sR - 2V_c + \Lambda)}. \quad (18)$$

Referring to Eq. 18, to ensure a stable system, we require  $\Lambda > 2V_c$ . This leads to what is known as the true PN guidance law shown in Eq. 19:

$$\bar{\mathbf{a}}_M \cdot \bar{\mathbf{I}}_n = NV_c \dot{\phi}_{\omega}, N > 2. \quad (19)$$

As is clear from the previous development, true PN commands missile acceleration normal to the LOS. This is, perhaps, more obvious by referring back to Eq. 13 and rewriting Eq. 19 as shown in Eq. 20:

$$\bar{\mathbf{a}}_{M_c} = NV_c \dot{\phi} \times \bar{\mathbf{I}}_r, N > 2. \quad (20)$$

Here,  $\bar{\mathbf{a}}_{M_c}$  represents commanded missile acceleration normal to the LOS. Achieved missile acceleration is physically realized through aerodynamic control surface deflections, control thruster operation, or a combination of both. Thus, Eq. 20 also emphasizes the fact that the development of PN assumes a no-lag missile response (i.e., the missile is assumed to respond instantly to, and achieve perfectly, the guidance command).

We will simply mention another variant of PN, referred to a pure proportional navigation (PPN). The names given to these variants are somewhat arbitrary, but these names have stuck. The general three-dimensional version of PPN can be expressed as shown in Eq. 21.

$$\bar{\mathbf{a}}_{M_c} = k \dot{\phi} \times \bar{\mathbf{v}}_M. \quad (21)$$

Here,  $k$  is the navigation gain. Clearly, PPN commands missile acceleration normal to the missile velocity vector,  $\bar{\mathbf{v}}_M$ .

In view of the importance of the PN law in missile guidance and space applications, considerable analytical study has been conducted regarding the behavior of a missile guided under PN. Since the differential equations governing PN motion, even when considering kinematics only, are highly nonlinear, only limited success has been achieved in solving these equations analytically.

## Mechanization of PN

Here, we discuss how PN can be mechanized in a homing missile. Central to this topic is the type of sensor that is used to detect and track the target: whether it is a passive (e.g., IR), semi-active, or active (e.g., RF or laser) sensor and, as important, how it is mounted to the missile.

As discussed, the conventional implementation of PN requires closing velocity and LOS rate information to produce the guidance (acceleration) commands. If we assume (for clarity) that the engagement is planar, then we can rewrite Eq. 20 as shown below, where  $\dot{\lambda}$  is the LOS rate in an inertial frame of reference:

$$a_{M_c} = NV_c \dot{\lambda}. \quad (22)$$

Thus, implementation of the PN guidance law in three dimensions dictates the necessity to measure LOS rate in two sensor instrument axes that are mutually perpendicular to the sensor boresight (near-coincident with the measured LOS to the target).

As mentioned previously, the way in which closing velocity ( $V_c$ ) and LOS rate ( $\dot{\lambda}$ ) information is obtained to mechanize PN guidance (Eq. 22) is a function of the type of target sensor that is used and how it is mounted to the missile body. Acquiring closing velocity information depends primarily on the target sensor type. Given an (onboard) active or semi-active RF system, for example, the observed Doppler frequency of the target return can be used to develop a good estimate of closing velocity,  $V_c$ . In other implementations, missile-to-target range or closing velocity can be periodically up-linked to the missile to facilitate PN guidance.

The way in which LOS rate ( $\dot{\lambda}$ ) information is derived depends on the type of target sensor that is used and how it is mounted to the missile. For example, a space-stabilized sensor (could be RF, IR, or laser) is mounted on a gimballed platform to increase the field of regard of the sensor and to isolate it from missile body motion. Conversely, tracking systems that do not require a large field of regard or that employ an IR focal plane array, for example, are fixed to the body (strapdown systems). Here, we will consider space-stabilized systems. Before introducing the details on how to derive LOS rate, we briefly discuss space-stabilized target sensor systems.

Various space-stabilized designs are possible, but a typical design is one in which two mutually perpendicular gimbals are employed along with rate gyros used for platform stabilization and LOS/LOS rate reconstruction. (Typically, these systems rely on the missile autopilot for roll stabilization.) Such gimballed platforms use a servomotor in each axis to accommodate seeker pointing. Hence, we will define a space-stabilized seeker to be composed of the target sensor (antenna/energy-collecting device and a receiver), gimbals (and associated servomotors), gyros, and the necessary control electronics. The necessary seeker functions are as follows: (i) track the target continuously after acquisition, (ii) provide a measure of the LOS angle ( $\lambda$ ) or LOS angular rate ( $\dot{\lambda}$ ), (iii) stabilize the seeker against significant missile body rate motion (pitching and yawing rate) that may be much larger than the LOS rate to be measured,



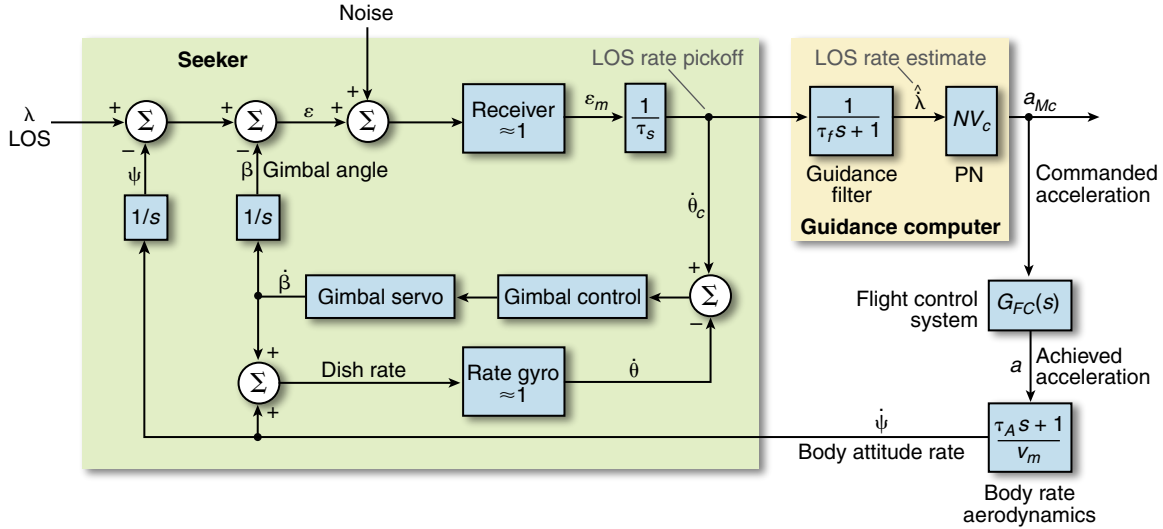


**Figure 5.** Simplified planar model of a traditional LOS rate reconstruction approach that directly supplies an LOS rate measurement to the guidance computer. Note that the LOS rate pickoff is assumed to be proportional to the boresight error measurement. The measured LOS rate is subsequently filtered to mitigate measurement noise and then applied to the PN homing guidance law.

Moreover, the transfer function from commanded acceleration (from the guidance law) to missile body rate ( $\dot{\psi}$ ) is approximated by the following aerodynamic transfer function, where  $\tau_A$  is the turning rate time constant and  $v_m$  is missile velocity:

$$\frac{\dot{\psi}}{a_c} = \frac{\tau_A s + 1}{v_m} \tag{26}$$

In this approach, the fact that the LOS rate is embedded in the tracking error ( $\epsilon_m$ ) is exploited. As illustrated, a LOS rate estimate is derived by appropriately filtering the receiver tracking error scaled by the seeker track-loop time constant.

Other approaches can be used to derive LOS rate for homing guidance purposes; these are generally referred to as either LOS reconstruction or LOS rate reconstruction. We next outline three alternative techniques (two LOS reconstructions and one LOS rate reconstruction).

**LOS Reconstruction**

As shown in Fig. 3, LOS reconstruction works to construct a measured LOS,  $\lambda_m$ , in an inertial frame of reference. The measured LOS then is filtered (via an appropriate guidance filter) to derive an estimate of LOS rate for guidance purposes. Two different LOS reconstruction approaches are as follows:<sup>9</sup>

1. Integrate the seeker gyro output and sum it with the measured tracking error. A block diagram of this approach is shown in Fig. 6. Mathematically, this approach can be expressed as Eq. 27:

$$\lambda_m = \epsilon_m + \int \dot{\theta} dt \tag{27}$$

2. Integrate the output of the missile body rate gyro, obtained from the missile IMU, and sum the integrated IMU gyro output together with the seeker gimbal angle and the measured tracking error. We illustrate this approach in the block diagram shown in Fig. 7. This approach is expressed mathematically as shown in Eq. 28:

$$\lambda_m = \epsilon_m + \beta + \int \dot{\psi} dt \tag{28}$$

From Fig. 3, it is clear that the two concepts are algebraically equivalent in the absence of noise and assuming perfect instruments (no gyro biases, drift, etc.); however, in practice, this is not the case. Moreover, we note that, in general, the guidance filters for the two approaches are not necessarily the same (e.g., for the simplified guidance filters shown in the figures, the filter time constants, represented by  $\tau_f$ , are not necessarily the same). The fundamentals of guidance filtering will be discussed in the companion article in this issue “Guidance Filter Fundamentals.” It is shown in Ref. 9 that the two LOS reconstruction approaches can yield significantly different results when noise and imperfect instruments are used. How these differences manifest themselves depends on the quality of the measurements and instruments that are used.

**LOS Rate Reconstruction**

A guidance signal also can be generated by differentiating the tracking error and adding it to the seeker rate gyro output. For practical purposes, taking the derivative of the tracking error is accom-

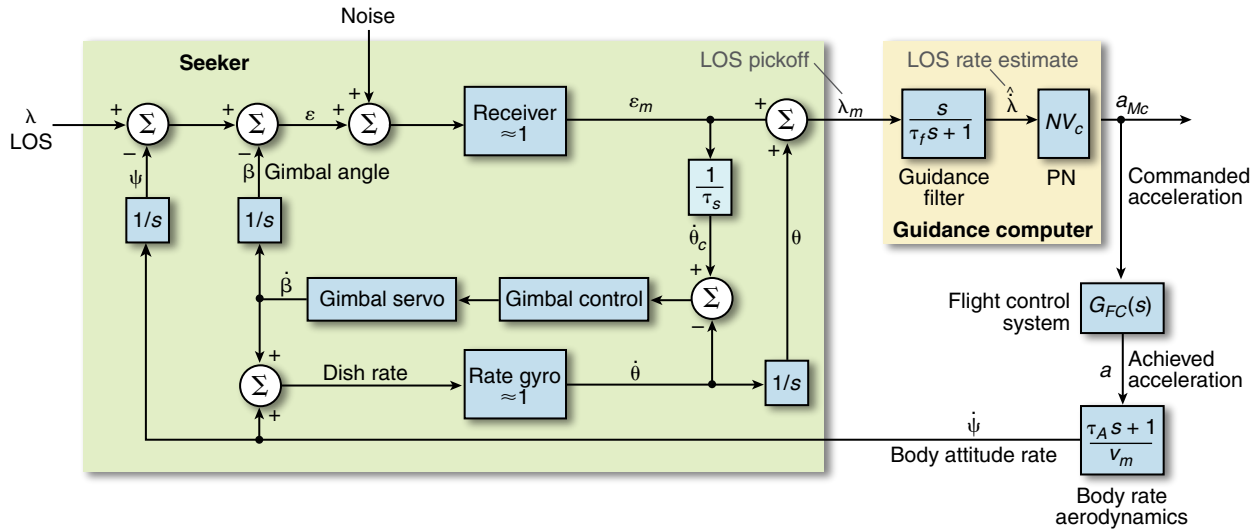


**Figure 6.** LOS reconstruction approach 1 wherein the seeker gyro output is integrated and summed with the measured tracking error to form an LOS measurement. The measured LOS is subsequently passed to the guidance computer, where it is filtered to extract an LOS rate and then applied to the PN guidance law.

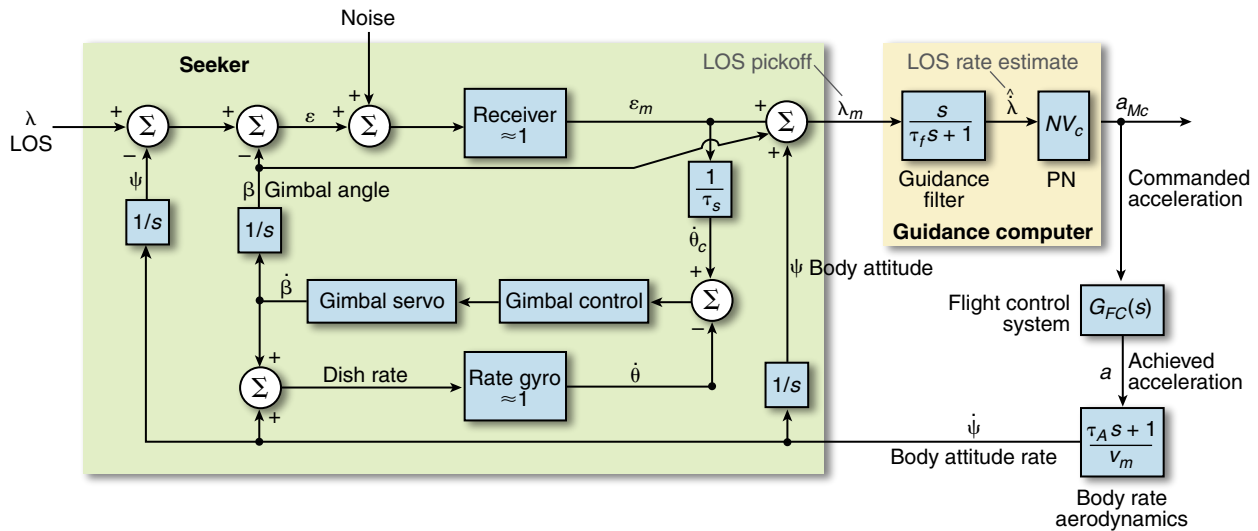


**Figure 7.** LOS reconstruction approach 2 wherein the output of the missile body rate gyro (via the missile IMU) is integrated and summed together with the seeker gimbal angle and the measured tracking error to develop an LOS measurement. The measured LOS is subsequently passed to the guidance computer, where it is filtered to extract an LOS rate and then applied to the PN guidance law.

plished by using a lead network such as that given below:

$$\frac{s}{\tau_D s + 1} \tag{29}$$

Figure 8 illustrates this approach. Here,  $\tau_D$  is the time constant of the lead network. As shown, the reconstructed LOS rate is filtered by an appropriate guidance filter (here represented by a simplified lag filter with time constant  $\tau_f$ ) to derive a LOS rate estimate. This method may lead to excessive amplification of the receiver noise

as a result of the differentiation process. However, in Ref. 10, it is shown that LOS rate reconstruction can work well if the missile turning rate (i.e., responsiveness to commands) is very fast.

### Radome/Irdome Design Requirements

In endoatmospheric engagements, a radome (or irdome) is required in order to protect the onboard seeker from the elements. For exoatmospheric vehicles, a radome/irdome is not necessarily required. The key dome requirements are summarized below<sup>8</sup>:



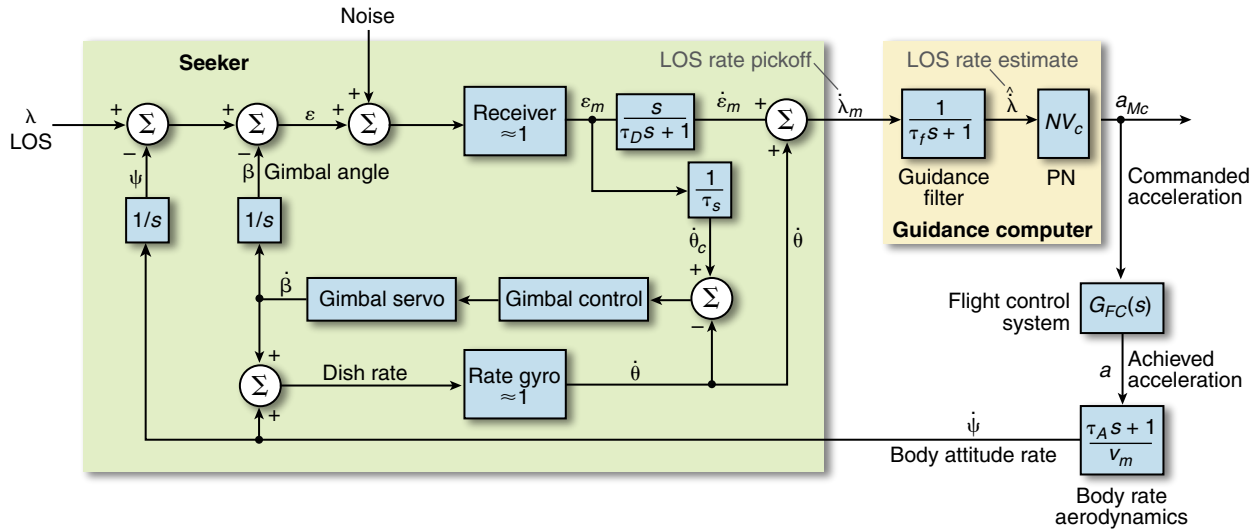


**Figure 8.** Simplified planar model of an alternate LOS rate reconstruction approach that can directly supply an LOS rate measurement to the guidance computer. Note that the LOS rate reconstruction differs between this figure and Fig. 5. As before, the measured LOS rate is subsequently filtered to mitigate measurement noise and then applied to the PN homing guidance law.

1. It must convey the energy with minimum loss.
2. It must convey the energy with minimum distortion, particularly angular distortion because this creates a parasitic feedback loop that can have a significant negative impact on guidance performance (discussed in more detail below).
3. It must have minimum aerodynamic drag.
4. It must have satisfactory physical properties, such as sufficient strength, resistance to thermal shock (from rapid aerodynamic heating), resistance to rain erosion at high speeds, and minimum water absorption.

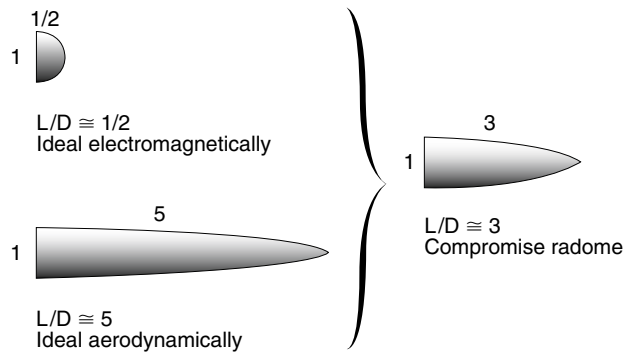


**Figure 9.** Three possible radome shapes are illustrated. For minimum angular distortion, a hemispherical shape (or hyper-hemispherical shape as in a ground-based radar) would be ideal electromagnetically (upper left), but the drag penalty is excessive. From an aerodynamic perspective, the lower left radome shape is preferable, but it tends to have significant angular distortion characteristics. The tangent-ogive shape (on the right) is a typical compromise design. Nevertheless, some missiles use much blunter dome designs despite the drag penalty. L/D, lift-to-drag ratio.

As an example, Fig. 9 illustrates three conceivable radome shapes. The tangent-ogive shape (on the right) is a typical compromise design.

### Guidance System Design Challenges

There are a significant number of challenges to designing guidance systems: the design must provide the desired performance while remaining robust to a multitude of error sources, limited control system bandwidth, and inherent system nonlinearities. Some of these challenges are summarized below.

1. The root-mean-square final miss distance from all deleterious noise sources must be minimized.
2. Guidance system stability must be maintained in the parasitic feedback loop (as mentioned above, this is caused by angular distortion of the radome/irdome). Radome angular distortion, in particular, is a key contributor to final miss distance but is considered separately from other noise sources as its impact on guidance system stability is substantial.
3. System nonlinearities must be avoided as much as possible; e.g., seeker gimbal angle and gyro rate saturations must be avoided, as should commanding missile acceleration beyond what is physically realizable by the missile.

### Contributors to Final Miss Distance

With respect to guidance challenge item 1 above, there are a number of contributors to final miss distance (other than angular distortion of the radome/irdome). For example, in either an RF or IR guidance system, measurement noise from the various instruments (onboard

seeker, IMU, etc.) will tend to increase the final miss distance. In a radar-guided system, high illumination power on the target is desired in order to reduce the necessary receiver gain and, consequently, the internally generated noise. Similarly, a passive IR seeker is designed to have a maximum aperture size to maximize incoming power. Therefore, antenna/aperture size usually is made a maximum within the constraint of missile body diameter to maximize power reception and minimize angular beam width, thereby leading to less noise.

The ability for any given target sensor to resolve closely spaced objects also is limited, contributing to additional miss distance. For example, a missile radar antenna usually has a relatively wide beamwidth, and so it is unable to resolve closely spaced targets in angle until very late in the endgame of the engagement. In this sort of ambiguous situation, the homing missile can incur a large final miss distance.

Some of the key contributors to final miss distance are introduced below<sup>8,11</sup>:

1. Seeker receiver range-dependent angle noise,  $\sigma_{rd}$ . This noise is a function of the strength of the target return power and, hence, the signal-to-noise ratio. Range-dependent noise power varies inversely with range to target ( $R$ ) as  $1/R^2$  for semi-active radar and as  $1/R^4$  for active radar. For IR systems, range-dependent angle noise typically is not considered to be a primary contributor.
2. Seeker range-independent angle noise,  $\sigma_{ri}$ . This noise is independent of target return power and is caused by a number of internal sources like signal processing and quantization effects, gimbal servo drive errors, and other electrical noise.
3. Scintillation (and glint) noise,  $\sigma_{glint}$ . These are coupled effects and are caused by target reflections that vary in amplitude and phase over time. (The effect is much like that of sunlight glinting from the shiny surfaces of an automobile.) Scintillation/glint noise can be very severe and is a function of the physical dimensions and motion of the target.
4. Clutter and multipath noise,  $\sigma_c$ . These noise effects become important at low altitudes, over either the land or sea. This noise is caused by the unwanted scattering (forward and backward) of radar returns from, for example, sea-surface waves.
5. Imperfect seeker stabilization caused by seeker gyro and gimbal scale factors, gyro drift, and missile body bending (flexing). Imperfect seeker stabilization can introduce parasitic feedback loops similar to that caused by radome/irdome distortion. The net effect can be viewed as inducing a bias or perturbation on the measured LOS rate. Exactly how these errors affect guidance performance will be a function of the way in which LOS reconstruction is mechanized.<sup>9</sup>
6. Initial heading errors at the start of homing. Heading error can be defined as the angle between the actual missile velocity vector at the start of terminal homing and the velocity vector that would be necessary to put the missile on an intercept course with the target. Heading error can be viewed as an initial condition disturbance to the guidance system at the start of terminal homing.
7. Target acceleration (maneuver) perpendicular to the LOS. A target can maneuver for any number of reasons (to avoid detection, to enact necessary course corrections, to evade a pursuing interceptor missile, etc.). Whatever the reason, from the viewpoint of the guided missile, target maneuver can have a stochastic quality to it and, in some instances, it can induce very large final miss distance. Relevant target maneuver (acceleration) levels and corresponding characteristics (horizontal weave, corkscrew, hard-turn, etc.) are key drivers to the design of missile guidance systems. Target maneuver generally is considered a (potentially significant) disturbance rather than noise to the guidance system.

Items 1–5 are stochastic noise sources, and the remaining items typically are referred to as non-noise contributors to final miss distance.

### Radome/Irdome Refraction Error

The ogival shape of radomes helps to reduce drag but is a significant source of trouble to guidance system performance. Irdome shapes tend to be less problematic than radome shapes, but their effect on guidance system performance still must be considered. The fundamental issue is that as radiation passes through the dome, it is refracted by a certain angle which, in turn, depends on the seeker look angle,  $\beta$ . As illustrated in Fig. 10,<sup>11</sup> the radome distorts the boresight error measurement by an amount  $\epsilon_{bse}$ . The magnitude of refraction during homing depends on many factors, including dome shape, fineness ratio, thickness, material, temperature, operating frequency, and polarization of the target return signal. Hence, it is very difficult to compensate perfectly for dome error *a priori*. Typically, the specification of dome characteristics involves the radome/irdome slope  $r$  (see Fig. 10), which is a local property of the dome and is defined as shown in Eq. 30:

$$r \equiv \frac{\partial \epsilon_{bse}}{\partial \beta} . \quad (30)$$

Although  $r$  is not a constant over the entire dome, it can be regarded as constant over a small range of seeker look angles,  $\beta$ . The most optimistic situation is one in which the designer would be able to specify the manufacturing tolerances and, thus, the limits on the allowable variations of  $r$ .

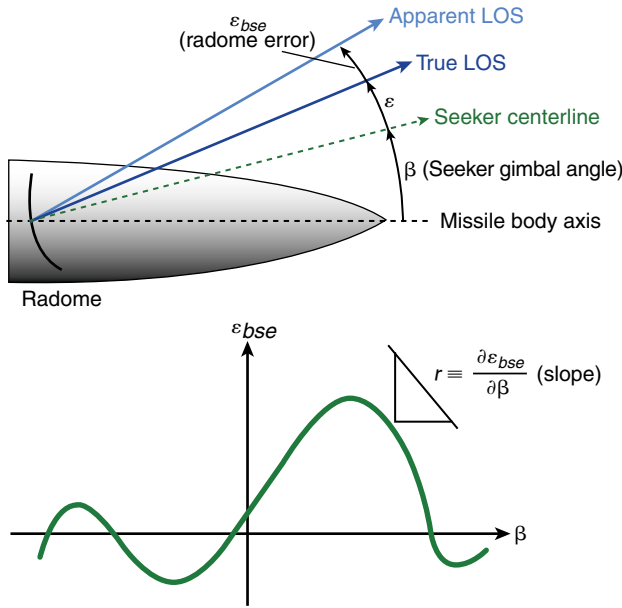


**Figure 10.** This illustration highlights the fact that the missile radome (or irdome) distorts the boresight error measurement. The boresight error distortion is a function of look angle.

Referring once again to Fig. 3, it follows that we can write the following angular relationship for the measured tracking error:

$$\varepsilon_m = \lambda + \varepsilon_{bse} - \theta. \quad (31)$$

Differentiating Eq. 31 and using the definition of radome slope shown in Eq. 30, we obtain the following expression for  $\dot{\varepsilon}_m$ :

$$\dot{\varepsilon}_m = \dot{\lambda} + \dot{\varepsilon}_{bse} - \dot{\theta} = \dot{\lambda} + r\dot{\beta} - \dot{\theta}. \quad (32)$$

Using the fact that the seeker dish angle can be written as  $\theta = \psi + \beta$ , we obtain the following expression for the derivative of the measured tracking error:

$$\dot{\varepsilon}_m = \dot{\lambda} - (1 - r)\dot{\beta} - \dot{\psi}. \quad (33)$$

Using Eq. 33, we can modify the block diagram shown in Fig. 5 to include the dome distortion effect (via Eq. 33). The result is shown in Fig. 11. Clearly, the boresight error creates another signal path in the missile guidance loop.

To obtain an alternate view of this parasitic loop and how it can affect guidance performance, we revisit Eq. 32. Referring to Fig. 3, we note that the seeker gimbal angle can be expressed as  $\beta = \theta - \psi$  and that the measured LOS can be written as  $\lambda_m = \theta + \varepsilon_m$ . Also noting that it is typical for  $|r| \ll 1$ , we can approximate Eq. 32 as

$$\dot{\lambda}_m \cong \dot{\lambda} - r\dot{\psi}. \quad (34)$$

Continuing, we also require transfer function descriptions of all components represented in Fig. 5. An approximate representation of the seeker block illustrated in Fig. 5 is given by the transfer function  $G_s(s)$  below:

$$G_s(s) \triangleq \frac{s\theta(s)}{\lambda(s)} = \frac{s}{\tau_s s + 1}. \quad (35)$$

Directly from Fig. 5, the combined guidance system (filter and law) transfer function can be expressed as

$$G_g(s) \triangleq \frac{a_{Mc}(s)}{s\lambda(s)} = NV_c G_F(s) = \frac{NV_c}{\tau_f s + 1}. \quad (36)$$

Next, we assume the transfer function from commanded to achieved missile acceleration,  $G_{FC}(s)$ , can be

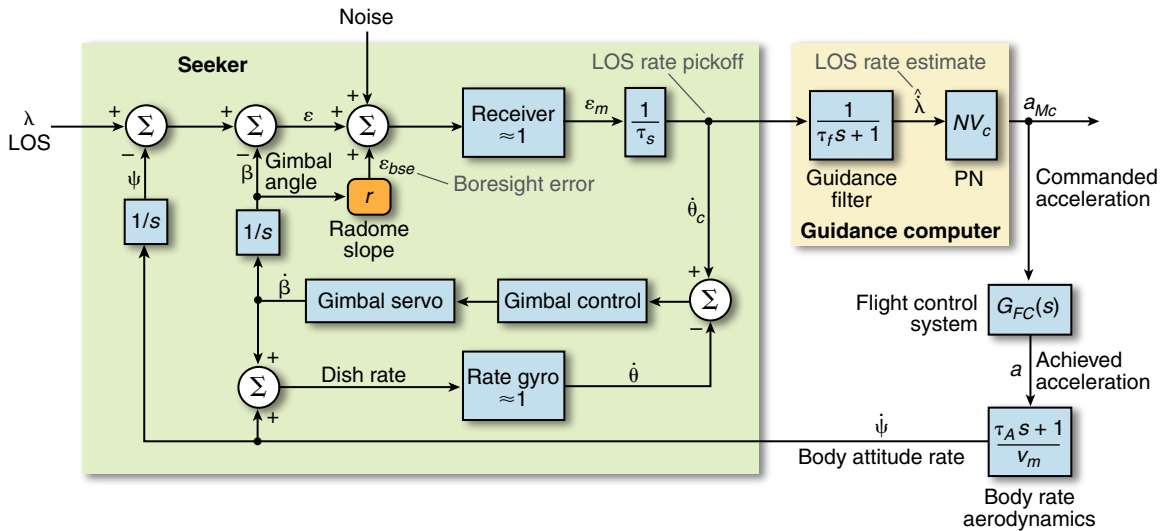


**Figure 11.** Simplified planar model of a gimballed seeker track loop with the inclusion of radome/irdome distortion effects on the measured boresight error.

approximated by the following first-order lag representation:

$$G_{FC}(s) \triangleq \frac{a_M(s)}{a_{Mc}(s)} = \frac{1}{\tau_{FC}s + 1}. \quad (37)$$

Finally, recall that the missile aerodynamic transfer function from acceleration to body rate can be approximated as shown in Eq. 26 and repeated here for convenience:

$$G_A(s) \triangleq \frac{s\psi(s)}{a_M(s)} = \frac{\tau_A s + 1}{v_m}. \quad (38)$$

Using Eqs. 34–38, Fig. 5 can be drawn as illustrated in Fig. 12. Referring to this block diagram, the closed-loop transfer function from LOS rate to missile acceleration can be written as

$$G_R(s) \triangleq \frac{a_M(s)}{s\lambda(s)} = \frac{NV_c G_F(s) G_{FC}(s) G_s(s)/s}{1 + \frac{rNV_c G_A(s) G_F(s) G_{FC}(s) G_s(s)}{sv_m}}. \quad (39)$$

**Static Effects**

Without refraction ( $r = 0$ ), the steady-state gain of the system in Eq. 39 is given by

$$g_{ss} \triangleq \lim_{s \rightarrow 0} G_R(s) \Big|_{r=0} = NV_c,$$

where recall that  $N > 2$ . On the other hand, if  $r \neq 0$ , then the steady-state gain of the system is given as

$$g_{ss} \triangleq \lim_{s \rightarrow 0} G_R(s) \Big|_{r \neq 0} = \frac{NV_c}{1 + r \frac{NV_c}{v_M}} \equiv \tilde{N}(r) V_c. \quad (40)$$

In Eq. 40, we have defined the resulting effective navigation ratio as  $\tilde{N}(r) = N/(1 + rNV_c/v_M)$ . Suppose the navigation ratio of the system is  $N = 3$  (for the  $r = 0$  case). Then, examining  $\tilde{N}(r)$ , if  $r$  is positive and (relatively) large and the ratio  $V_c/v_M$  increases beyond unity (as is often the case, particularly for near head-on

engagements), then the effective navigation ratio  $\tilde{N} \rightarrow 2$ . Recall from the discussion of PN that a navigation gain of 2 or less will lead to guidance instability. This fact is illustrated in Fig. 13 for  $N = 3$  and three different ratios of  $V_c/v_M$ . Conversely, when  $r$  is negative, the effective navigation ratio  $\tilde{N}$  will increase, resulting in additional noise throughput, which also can have detrimental effects on guidance performance.

**Dynamic Effects**

It is shown in Ref. 4 that the guidance system transfer function given by Eq. 39 and illustrated in Fig. 12 can be approximated further by the following simplified transfer function:

$$G_R(s) \triangleq \frac{a_M(s)}{s\lambda(s)} \cong \frac{NV_c}{1 + \rho} \frac{1}{1 + s\tau_R}. \quad (41)$$

In Eq. 41,  $\rho = rNV_c/v_M$ , and the approximate overall time constant,  $\tau_R$ , is given by the composite expression in Eq. 42:

$$\tau_R = \frac{(\tau_s + \tau_f + \tau_{FC}) + \rho\tau_A}{1 + \rho}. \quad (42)$$

Referring to Eqs. 41 and 42, when the dynamic pressure is low (e.g., high altitudes and/or low missile velocity), the aerodynamic time constant  $\tau_A$  tends to take on relatively large values (the missile turning rate becomes sluggish). For positive values of  $\rho$ , this effect is exacerbated and the missile guidance loop becomes even more sluggish. On the other hand, when the dynamic pressure is low, large negative values of  $\rho$  coupled with large  $\tau_A$  can induce guidance instability.

As an example, consider Fig. 14, which illustrates the deleterious effects of radome-induced boresight error on homing guidance performance. This example uses PN guidance to guide the missile against a non-maneuvering target. No other noise sources are considered other than radome boresight error. Several curves are shown, each representing an autopilot response capability given by the time constant  $\tau = \tau_{FC}$ . Clearly, a more sluggish time constant exacerbates the effects of radome error slope on homing performance.

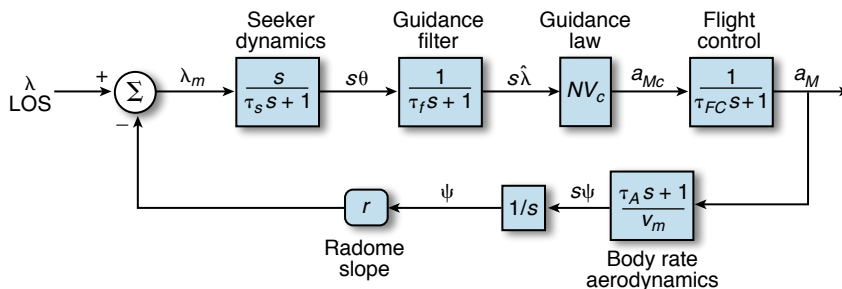


**Figure 12.** Alternate simplified block diagram of a (linear) missile guidance and control system that accounts for seeker dynamics, radome distortion, guidance filter effects, and autopilot/airframe response characteristics.

**Guidance System Nonlinearities**

In a guided missile, there are limits to the region of linear operation. For example, the lateral acceleration that a guided missile can attain is limited in one of two ways: (i) for low-altitude intercepts, structural considerations will limit the maximum acceleration levels, and (ii) for high-altitude intercepts, the

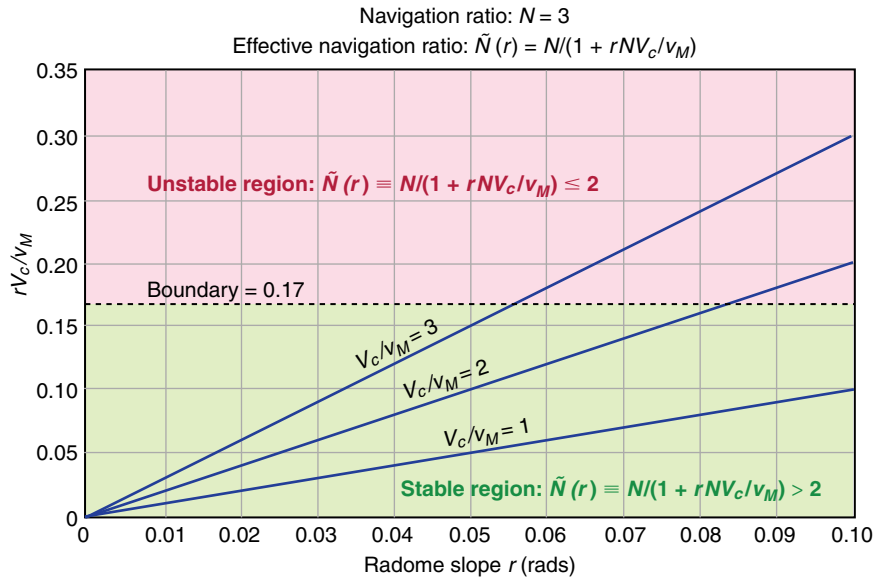


**Figure 13.** For a navigation ratio of 3, the effect of positive radome boresight error slope ( $r$ ) for increasing ratios of closing velocity over missile velocity is shown. To maintain guidance stability, the effective navigation ratio must remain greater than 2.

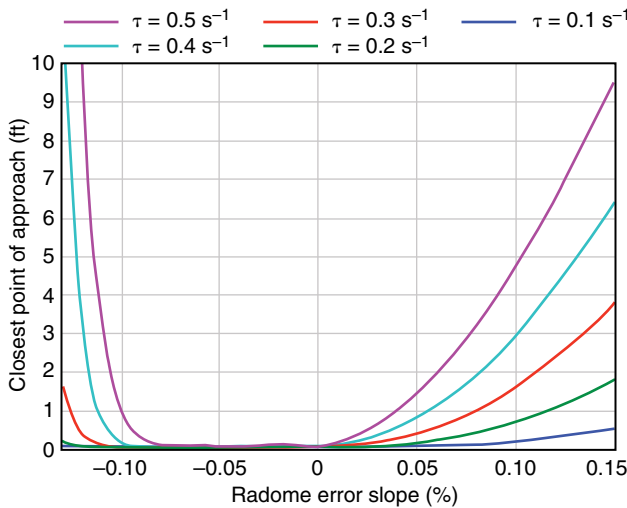


**Figure 14.** This plot illustrates the miss performance of PN versus radome boresight error slope. The results were derived by using a planar Simulink model assuming no error sources aside from radome error. Each curve represents the results using an autopilot with specified time constant  $\tau$ . A larger time constant indicates a larger lag in the missile response to acceleration commands.

acceleration limit is more a result of maximum angle-of-attack limitations. In either case, the missile guidance and control system design must take the acceleration limits into account. The most significant implication is that the commanded acceleration from the guidance system must be hard-limited so as not to exceed the acceleration limits of the missile, which also implies

that the flight control system (autopilot) must be designed to produce minimum overshoot to an acceleration step command. If/when the guidance command saturates, the missile guidance loop is essentially opened. If guidance command saturation persists long enough, and if this persistent saturation occurs near intercept, a significant final miss distance can result.

Missile seeker systems also are prone to nonlinear saturation, which can have significant deleterious effects on overall guidance performance. For example, on gimballed platforms, the seeker gimbal angle can saturate under certain stressing conditions (e.g., while pursuing a highly maneuvering target). If this saturation occurs, the guidance loop has

effectively become open and, if this occurs near intercept, significant final miss distance can occur.

### Guidance Command Preservation

Three-dimensional guidance laws usually generate a guidance command vector without consideration to how the missile interceptor will effectuate the specified maneuver. For example, it is typical for a guided missile to (i) have no direct control over its longitudinal acceleration (e.g., axial thrust is not typically throttleable) and (ii) maneuver in the guidance direction (specified by the guidance law) by producing acceleration normal to the missile body. Therefore, the question naturally arises as to how a three-dimensional guidance command, specified by the guidance law without consideration of the aforementioned constraints, can be achieved by maneuvering the missile perpendicular to the missile centerline. We shall refer to this process as guidance command preservation.

In Ref. 1, two guidance command preservation techniques are developed. The first approach, referred to here as GCP1, is further elaborated in Ref. 12. The second guidance command preservation technique (GCP2) is a minimum norm solution. As such, GCP2 could (theoretically) provide savings in commanded acceleration (or fuel use in exoatmospheric applications) as compared with the first method. The GCP1 technique is discussed here.

### GCP1 Technique

To describe this guidance command preservation technique, we refer to Fig. 15 and make the following



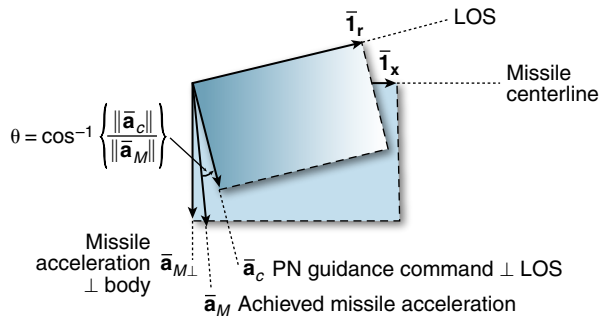


**Figure 15.** GCP1. The LOS vector is shown along with the commanded acceleration from PN, which is perpendicular to the LOS. Also, the missile centerline (direction of the missile nose) and achieved missile acceleration vector are superimposed. The guidance preservation problem is to achieve missile acceleration that has the component along the guidance direction as specified by the guidance law.

definitions:  $\bar{1}_r$  is a unit vector along the missile–target LOS,  $\bar{1}_x$  is a unit vector along the missile centerline (missile longitudinal axis),  $\bar{a}_c$  is the guidance law acceleration command perpendicular to the LOS, and  $\bar{a}_M = [a_{Mx} \ a_{My} \ a_{Mz}]^T$  is the achieved missile acceleration vector comprising components in the  $x/y/z$  axes.

Two component directions serve as a basis for the development of GCP1: the direction of the LOS ( $\bar{1}_r$ ) and the commanded guidance direction ( $\bar{1}_{a_c} = \bar{a}_c / \|\bar{a}_c\|$ ). Assuming perfect interceptor response to commanded acceleration (i.e., no lag from commanded to achieved acceleration), the (guidance preserved) missile acceleration can be expressed as follows:

$$\bar{a}_M = k_1 \bar{1}_r + k_2 \bar{1}_{a_c}. \quad (43)$$

The design parameters,  $k_1$  and  $k_2$ , are determined subject to the following constraints:

$$\begin{aligned} \bar{a}_M \cdot \bar{1}_x &= a_{Mx} \\ \bar{a}_M \cdot \bar{1}_{a_c} &= \|\bar{a}_c\|. \end{aligned} \quad (44)$$

Equations 44 analytically embody the following constraints: (i) the missile does not control longitudinal acceleration and (ii) the component of missile acceleration along the guidance direction,  $\bar{1}_{a_c}$ , must be that specified by the guidance law ( $\bar{a}_c$ ). Using Eqs. 43 and 44 and given  $\bar{1}_r \cdot \bar{1}_{a_c} = 0$  (i.e., the guidance command is perpendicular to the LOS), an expression for commanded missile acceleration that will preserve the guidance command is given in Eq. 45:

$$\bar{a}_{GL} = \left( \frac{a_{Mx} - \bar{a}_c \cdot \bar{1}_x}{\bar{1}_r \cdot \bar{1}_x} \right) \bar{1}_r + \bar{a}_c. \quad (45)$$

Equation 45 is derived independently from any particular coordinate system. It is easy to mechanize the expression in Eq. 45 such that the computations are carried out in the missile body frame (B). We first note that missile acceleration resolved into the missile body frame can be expressed as  $\bar{a}_M^B = [a_{Mx}^B \ a_{My}^B \ a_{Mz}^B]^T$  and that the body-referenced unit vector along the longitudinal axis of the missile can be written as  $\bar{1}_x^B = [1 \ 0 \ 0]^T$ . The quantities  $\bar{1}_r$  (LOS unit vector) and  $\bar{a}_c$  (guidance law command) usually are defined with respect to a guidance reference frame. To reflect this fact, we express them as  $\bar{1}_r^G = [1 \ 0 \ 0]^T$  and  $\bar{a}_c^G = [0 \ a_{cy}^G \ a_{cz}^G]^T$ . Here, the superscript denotes the frame of reference with which the quantities are currently expressed; in this case, the guidance reference frame (G). Thus, we must resolve all guidance frame quantities into the missile body frame through the coordinate transformation  $C_G^B = c_G^B(i, j)$ ,  $i, j = 1, 2, 3$ ; for example,  $\bar{1}_r^B = C_G^B [1 \ 0 \ 0]^T \equiv [c_G^B(1, 1) \ c_G^B(2, 1) \ c_G^B(3, 1)]^T$ . Note that if we fix the guidance frame at the start of terminal homing ( $t = 0$ ), we obtain the transformation  $C_I^G = C_I^B (C_B^S|_{t=0})$ . The inertial-to-body transformation,  $C_I^B$ , comes from the IMU, and  $C_B^S$  may be computed via the seeker gimbals (see Eq. 23). Subsequently,  $C_G^B = C_I^B (C_I^G)^T$ . If necessary, the guidance frame may be updated from instant to instant, but this adds computational complexity. Given that  $C_G^B$  is available, the following mechanization of Eq. 45 is possible:

$$\begin{aligned} \bar{a}_{GC}^B &= \left( \frac{a_{Mx}^B - \bar{a}_c^B \cdot \bar{1}_x^B}{\bar{1}_r^B \cdot \bar{1}_x^B} \right) \bar{1}_r^B + \bar{a}_c^B \\ &\equiv \left( \frac{a_{Mx}^B - a_{cx}^B}{c_G^B(1, 1)} \right) \begin{bmatrix} c_G^B(1, 1) \\ c_G^B(2, 1) \\ c_G^B(3, 1) \end{bmatrix} + \begin{bmatrix} a_{cx}^B \\ a_{cy}^B \\ a_{cz}^B \end{bmatrix}. \end{aligned} \quad (46)$$

In Eq. 46,  $[a_{cx}^B \ a_{cy}^B \ a_{cz}^B]^T$  is the guidance command vector expressed in the missile body frame. This mechanization will generate guidance commands in the missile body frame that satisfy the constraints in Eq. 44.

## MIDCOURSE GUIDANCE

So far, this article has been chiefly concerned with the requirements of terminal homing, wherein target measurements are provided by one or more onboard terminal sensors and minimizing miss distance at intercept is the primary objective. For completeness' sake, we now will briefly discuss issues and requirements associated with the midcourse phase of flight.

During the midcourse guidance phase of a multi-mode missile (see Fig. 16), target tracking is performed by an external sensor to support the engagement.<sup>6</sup> External tracking relaxes the requirements for the onboard sensor to point at the target and detect it at large ranges.

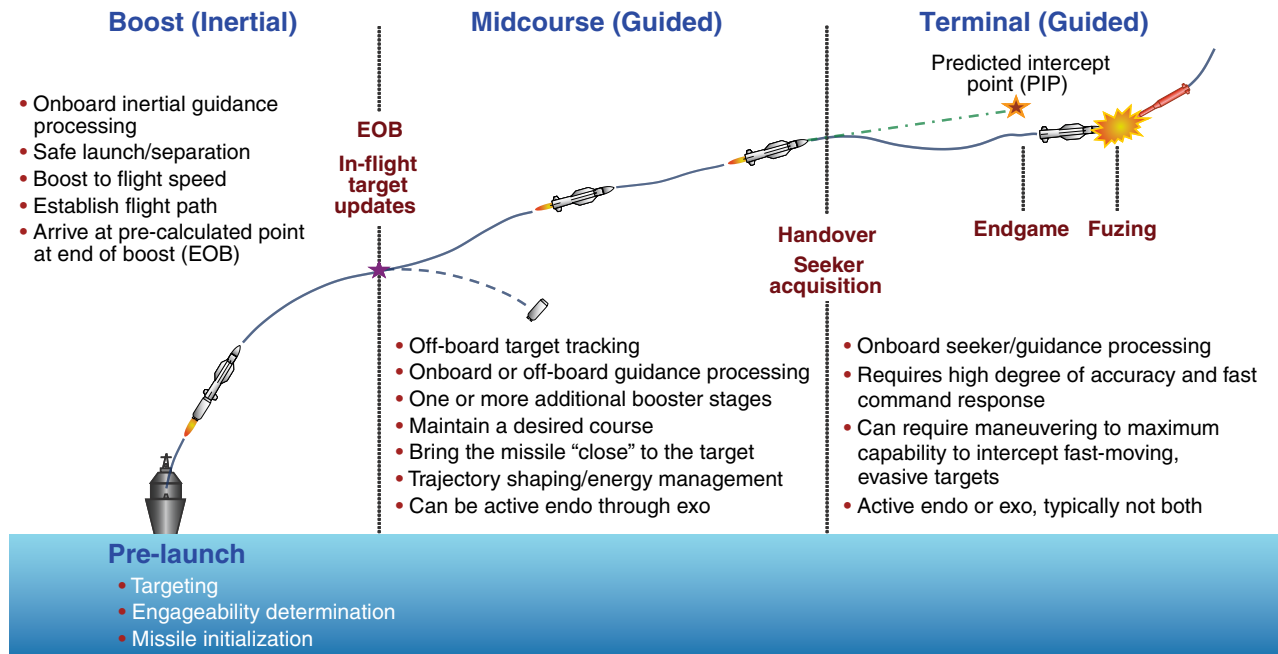


**Figure 16.** Missile guidance phases. The weapon control system first decides whether the target is engageable. If so, a launch solution is computed and the missile is initialized, launched, and boosted to flight speed. Inertial guidance typically is used during the boost phase of flight during which the missile is boosted to flight speed and roughly establishes a flight path to intercept the target. Midcourse guidance is an intermediate flight phase whereby the missile receives information from an external source to accommodate guidance to the target. During the midcourse phase, the missile must guide to come within some reasonable proximity of the target and must provide desirable relative geometry against a target when seeker lock-on is achieved (just prior to terminal homing). The terminal phase is the last and, generally, the most critical phase of flight. Depending on the missile capability and the mission, it can begin anywhere from tens of seconds down to a few seconds before intercept. The purpose of the terminal phase is to remove the residual errors accumulated during the previous phases and, ultimately, to reduce the final distance between the interceptor and target below some specified level.

However, the accuracy of sensors generally degrades with distance. It is therefore unlikely that a standoff sensor will have sufficient accuracy in tracking both the target and missile to guide a missile close enough for intercept. The objectives during midcourse guidance are instead to guide the missile to a favorable geometry with respect to the target for both acquisition by the onboard sensor and handover to terminal homing.

During the midcourse guidance phase, the weapon control must provide information to the missile about the threat. This information may be nothing more than estimates of the threat kinematic states or may include a predicted intercept point (PIP). Predictions of the future target trajectory, whether calculated on board the missile or by the weapon control system, are based on assumptions of what maneuvers the threat is likely to do and what maneuvers are possible for the threat to perform. These assumptions typically are sensitive to the type of threat assumed but may include booster profiles, aerodynamic maneuverability, or drag coefficient(s). The PIP is therefore highly prone to errors. Occasional in-flight target updates may be needed to improve the accuracy of the PIP before handover to terminal homing.

A form of PN might be used during the midcourse guidance phase but generally results in excessive slow-down, however, as a result of the added atmospheric drag generated by maneuvers. Instead, it is desirable to use a guidance law that will maximize missile velocity during the endgame such that missile maneuverability will be maximized when called for during stressing endgame maneuvers. Lin<sup>11</sup> describes an approach that applies optimal control theory to derive efficient, analytical solutions for a guidance law that approximately maximizes the terminal speed while minimizing the miss distance. The guidance commands are expressed in the form given in Eq. 47:

$$a = \frac{K_1}{R} V^2 \sin(\delta) \cos(\sigma) - \frac{K_2}{R} V^2 \sin(\sigma). \quad (47)$$

Here,  $V$  is the missile speed,  $R$  is the range to the PIP,  $\delta$  is the angle difference between the current and desired final velocity, and  $\sigma$  is the heading error. The first term shapes the trajectory to achieve a desired approach angle to the intercept, and the second term minimizes miss. The gains  $K_1$  and  $K_2$  are time-varying

and depend on flight conditions, booster assumptions, and other factors. A critical component of implementing this law is computing an accurate estimate of time-to-go when the missile is still thrusting, which depends on the component of missile acceleration along the LOS. The guidance calculations can be made on board the missile or off board, with acceleration commands passed from the weapon control system to the missile where they are converted to body coordinates.

For exoatmospheric flight, drag is no longer an issue, but long flight times will result in curved trajectories as a result of gravity. From the current position, the Lambert solution (see Ref. 7 for a simple synopsis) defines the necessary current velocity to reach a terminal intercept point at a given time. A guidance law can be “wrapped around” the Lambert solution to progressively steer the missile velocity vector to align with the Lambert velocity. Then either thrust termination or a slow-down maneuver can be used to match the magnitude of the velocity of the Lambert solution when the missile booster burns out.

## CLOSING REMARKS

The key objective of this article was to provide a relatively broad conceptual foundation with respect to homing guidance but also of sufficient depth to adequately support the articles that follow. First, we discussed handover analysis and emphasized that the displacement error between predicted and true target position,  $\bar{\mathbf{e}}$ , can be decomposed into two components: one along ( $\bar{\mathbf{e}}_{\parallel}$ ) and one perpendicular to ( $\bar{\mathbf{e}}_{\perp}$ ) the predicted LOS. Thus, because the relative velocity is along the LOS to the predicted target location, the error along this direction alters the time of intercept but does not contribute to the final miss distance. It is the error perpendicular to the LOS that must be removed by the interceptor after transition to terminal homing to effect an intercept.

Next, we developed a classical form of PN and noted that a primary advantage of PN, contributing to its longevity as a favored guidance scheme over the last five decades, is its relative simplicity of implementation. In fact, the most basic PN implementations require low levels of information regarding target motion as compared with other, more elaborate schemes, thus simplifying onboard sensor requirements. Moreover, it has proven to be relatively reliable and robust. This particular (and somewhat unique) treatment of PN was taken from a 1980 APL memorandum written by Alan J. Pue.<sup>1</sup> We also discussed how PN can be mechanized for guided

missile applications, with a focus on LOS reconstruction and guidance command preservation. With respect to homing guidance, we itemized the primary contributors to guidance performance degradation that can ultimately lead to unacceptable miss distance.

The onboard missile seeker has a limited effective range beyond which target tracking is not possible. To support engagements that initially are beyond such a range, midcourse guidance is used to bring the missile within the effective range of the seeker. Thus, in contrast to terminal homing, during the midcourse guidance phase of flight, the target is tracked by an external sensor and information is uplinked to the missile. The key objectives during midcourse guidance are to guide the missile to a favorable geometry with respect to the target for both acquisition by the onboard missile targeting sensor and to provide acceptable handover to terminal homing. Many of the terminal homing concepts discussed here and in the subsequent articles on modern guidance and guidance filtering in this issue also are applicable to developing midcourse guidance policies. Thus, mainly for completeness, we briefly introduced the problem of midcourse guidance.

## REFERENCES

- <sup>1</sup>Pue, A. J., *Proportional Navigation and an Optimal-Aim Guidance Technique*, Technical Memorandum FIC(2)80-U-024, JHU/APL, Laurel, MD (7 May 1980).
- <sup>2</sup>Ben-Asher, J. Z., and Yaesh, I., *Advances in Missile Guidance Theory*, American Institute of Aeronautics and Astronautics, Reston, VA (1998).
- <sup>3</sup>Locke, A. S., *Principles of Guided Missile Design*, D. Van Nostrand Company, Princeton, NJ (1955).
- <sup>4</sup>Shneydor, N. A., *Missile Guidance and Pursuit: Kinematics, Dynamics and Control*, Horwood Publishing, Chichester, England (1998).
- <sup>5</sup>Shukala, U. S., and Mahapatra, P. R., “The Proportional Navigation Dilemma—Pure or True?” *IEEE Trans. Aerosp. Electron. Syst.* **26**(2), 382–392 (Mar 1990).
- <sup>6</sup>Witte, R. W., and McDonald, R. L., “Standard Missile: Guidance System Development,” *Johns Hopkins APL Tech. Dig.* **2**(4), 289–298 (1981).
- <sup>7</sup>Zarchan, P., *Tactical and Strategic Missile Guidance*, 4th Ed., American Institute of Aeronautics and Astronautics, Reston, VA (1997).
- <sup>8</sup>Stallard, D. V., *Classical and Modern Guidance of Homing Interceptor Missiles*, Raytheon Report D985005, presented at an MIT Dept. of Aeronautics and Astronautics seminar (Apr 1968).
- <sup>9</sup>Miller, P. W., *Analysis of Line-of-Sight Reconstruction Approaches for SM-2 Block IVA RRFD*, Technical Memorandum FIE(94)U-2-415, JHU/APL, Laurel, MD (22 Dec 1994).
- <sup>10</sup>Nesline, F. W., and Zarchan, P., “Line-of-Sight Reconstruction for Faster Homing Guidance,” *AIAA J. Guid. Control Dyn.* **8**(1), 3–8 (Jan–Feb 1985).
- <sup>11</sup>Lin, C. F., *Modern Navigation, Guidance, and Control Processing*, Prentice Hall, Englewood Cliffs, NJ (1991).
- <sup>12</sup>Abedor, J. L., *Short Range Anti-Air Warfare Engagement Simulation*, Technical Memorandum FIE(86)U-3-031, JHU/APL, Laurel, MD (10 Nov 1986).

# The Authors

**Neil F. Palumbo** is a member of APL's Principal Professional Staff and is the Group Supervisor of the Guidance, Navigation, and Control Group within the Air and Missile Defense Department (AMDD). He joined APL in 1993 after having received a Ph.D. in electrical engineering from Temple University that same year. His interests include control and estimation theory, fault-tolerant restructurable control systems, and neuro-fuzzy inference systems. Dr. Palumbo also is a lecturer for the JHU Whiting School's Engineering for Professionals program. He is a member of the Institute of Electrical and Electronics Engineers and the American Institute of Aeronautics and Astronautics.

**Ross A. Blauwkamp** received a B.S.E. degree from Calvin College in 1991 and an M.S.E. degree from the University of Illinois in 1996; both degrees are in electrical engineering. He is pursuing a Ph.D. from the University of Illinois. Mr. Blauwkamp joined APL in May 2000 and currently is the supervisor of the Advanced Concepts and Simulation Techniques Section in the Guidance, Navigation, and Control Group of AMDD. His interests include dynamic games, nonlinear control, and numerical methods for control. He is a member of the Institute of Electrical and Electronics Engineers and the American Institute of Aeronautics and Astronautics.

**Justin M. Lloyd** is a member of the APL Senior Professional Staff in the Guidance, Navigation, and Control Group of AMDD. He holds a B.S. in mechanical engineering from North Carolina State University and an M.S. in mechanical engineering from Virginia Polytechnic Institute and State University. Currently, Mr. Lloyd is pursuing his Ph.D. in electrical engineering at The Johns Hopkins University. He joined APL in 2004 and conducts work in optimization; advanced missile guidance, navigation, and control; and integrated controller design. For further information on the work reported here, contact Neil Palumbo. His email address is [neil.palumbo@jhuapl.edu](mailto:neil.palumbo@jhuapl.edu).



Neil F. Palumbo



Ross A. Blauwkamp



Justin M. Lloyd

The Johns Hopkins APL Technical Digest can be accessed electronically at [www.jhuapl.edu/techdigest](http://www.jhuapl.edu/techdigest).